

Electronic Toll Collection Using Portable RFID TAG with Antitheft System

S. P. Edison, M. Kirubahar, R. Nandhakumar, T. K. Naveenraj

Department of Electronic and Communication Engineering, K. Ramakrishnan College of Technology, India

Article Info

Article history:

Received 14 February 2015

Received in revised form

20 February 2015

Accepted 28 February 2015

Available online 6 March 2015

Keywords

Electronic toll collection (ETC),
Global Navigation Satellite Systems
(GNSS),

Receiver Autonomous Integrity

Abstract

Electronic toll collection (ETC) systems based on user position estimated with Global Navigation Satellite Systems (GNSS) are particularly attractive due to their exibility and reduced roadside infrastructure in comparison to other systems such as tollbooths. Because GNSS positioning may be perturbed by different errors and failures, ETC systems, as liability critical applications should monitor the integrity of GNSS signals in order to limit the use of faulty positions and the consequent charging errors. The integrity-monitoring systems have been originally designed for civil aviation monitoring (RAIM), urban environment. This paper studies the use of receiver autonomous integrity monitoring (RAIM), which are algorithms run within the GNSS receiver and, therefore, are easier to tune to ETC needs than other systems based on external information. It also have an anti Theft system works based on gps and rfid tag which track the location simulataneously. user can get the location by sending a key message to Gsm module fixed at vehicle. vehicle engine starting can be also controlled By using this gsm system.

1. Introduction

INTEGRITY of Global Navigation Satellite Systems (GNSS) is defined as a measure of the trust that can be placed in the correctness of the information supplied by the navigation system [1]. The concept of GNSS integrity was originally developed in the civil aviation framework as part of the International Civil Aviation Organization (ICAO) requirements for using GNSS in the communications, Navigation, and Surveillance/Air Traffic Management system. In particular, civil aviation standards specify a set of minimum accuracy, availability, integrity, and continuity performance on the GNSS signal-in-space (SIS) for each operation and phase of flight [2]. Nevertheless, a standalone GPS cannot meet the stringent civilaviation requirements, and, specifically, the GPS SIS integrity standard [3] does not assure integrity as specified by the ICAO. For this reason, various augmentation systems have been developed to allow the use of GPS within the ICAO requirements. These systems are classified according to their infrastructure into Ground-, Satellite-, and Aircraft-Based Augmentation Systems (GBAS, SBAS and ABAS).

The need for reliable satellite navigation with integrity monitoring is not limited to the civil aviation field. Two types of applications need GNSS integrity, i.e., safety-of-life applications, in which undetected navigation errors may endanger life, and liability critical applications, in which positioning errors may have negative legal or economic consequences [4]. A number of integrity-driven positioning applications have vehicular or pedestrian users and take place in urban and rural environments [5]. A few examples of these applications are electronic toll collection (ETC), train control, dangerous or valuable goods transport survey, and emergency calls.

Each application has its own integrity constraints and needs an integrity-monitoring technique adapted to its

specifications. This paper focuses on ETC systems in urban and rural environments based on GNSS positioning. GNSS-based ETC schemes are particularly interesting because they are free-flow (payas-you-drive) highly flexible systems with a reduced quantity of roadside infrastructure. Moreover, satellite navigation is, together with 5.8-GHz microwave and GSM-GPRS communication systems, one of the technologies the European Union recommends for the European Electronic Toll Service [6]. As of 2012, toll systems for freight transport using GPS as primary positioning technology are already operational in German and Slovak highways and national roads [7], [8].

GNSS-based ETC systems are liability-critical applications because excessive and uncontrolled positioning errors may lead to incorrect toll invoices. The act of levying a toll lower than it should be is denoted as undercharging and implies a loss of revenue, whereas the act of levying a toll higher than it should be is known as overcharging and may originate user claims. Thus, ETC specifications should bind the maximum acceptable rate of undercharging and overcharging errors in order to assure the quality of service to both users and the toll operator. For this reason, GNSS integrity monitoring is a key element of ETC systems, which assures that positioning errors are below the specified limits, detecting unacceptably large errors. Different solutions have been studied to monitor the navigation integrity in urban environments, often hybridizing GNSS with dead-reckoning and map-matching techniques [9]–[11]. The aim of this paper is to present an integrity-monitoring algorithm that only uses GNSS measurements, consisting of a snapshot RAIM tailored to the needs of ETC in urban environments. This approach reduces the complexity of the on-board equipment and avoids memory problems due to error propagation in recursive loops, as well as the thorough characterization of errors due to non-GNSS components required by integrity mechanisms. The least squares residual (LSR) RAIM has been chosen because it is well known in civil aviation and is commonly

Corresponding Author,

E-mail address: naveeneceraja@gmail.com

All rights reserved: <http://www.ijari.org>

taken as a baseline algorithm [12]. A digital map is used to charge the user, but not in the integrity-monitoring process. This paper is organized as follows: First, the GNSS based ETC scheme with integrity monitoring is explained in Section II. Afterward, the weighted LSR (WLSR) RAIM used in civil aviation and a modified version adapted to the ETC needs in urban environments are analyzed in Sections III and IV. The characteristics of both RAIM algorithms are compared in Section V, and, finally, Section VI presents their performance calculated via simulations.

2. GNSS-Based Etc Systems

The discrete road links charging toll scheme defined in the ISO standard [13] is studied. The geo-fencing approach is followed, in which the tolled road network is split into segments defined by virtual perimeters. The areas within the perimeters are denoted geo-objects and constitute the basic charging units, that is, users are charged the price associated to a geo-object whenever they are detected inside it. Each geo-object's fee is individually set and can be designed according to different factors such as the user category, the time of the day, or the traffic state. Moreover, distance-based charge is possible when geoobjects are defined as road portions between intersections, with only one entrance and one exit. Geo-fencing is an appropriate approach for GNSS-based ETC applications that allows highly flexible systems with a low number of roadside infrastructures. The main task of the ETC system is to decide whether a user has driven through a road segment or not and charge him if he has. This decision, which is known as geo-object recognition, can be taken as a function of the number of user positions lying inside the geo-object boundaries. In order to bind the maximum rate of erroneous geo-object recognitions (i.e., erroneously charged segments), only positions declared valid by the integrity-monitoring system are used. Moreover, only independent positions are taken to eliminate the effects of the positioning error temporal correlation. In this context, two position estimates are independent when they produce independent integrity-monitoring outputs. The correlation time depends on the GNSS receiver type and other constraints within the local environment. Summarizing, the proposed road segment charging algorithm is charge segment \Leftrightarrow Nvalid INSIDE \geq NTh (1) where Nvalid INSIDE is the number of valid and independent positions inside the geo-object, and NTh is the geo-object recognition threshold. The integrity-monitoring systems have been originally designed to meet the civil aviation requirements; hence, they need to be adapted to the ETC specifications. From the various possible integrity-monitoring systems, this work receiver autonomous integrity monitoring (RAIM), which are algorithms run within the GNSS receiver that monitor integrity due to redundant pseudorange measurements. Since RAIM algorithms, as opposed to GBAS or SBAS, do not rely on external information, they can be easily adapted to the ETC requirements and to the multifrequency multiconstellation case. This paper considers the use of SBAS corrections but not of its integrity service because it has been designed mainly to assure the civil aviation requirements. Only the integrity of horizontal positioning is required to be monitored for ETC application. For each estimated position, RAIM provides a horizontal protection level (HPL), which

is defined as a circular area centered at the user real position that is assured to contain the estimated position with a probability that is equal to or higher than $(1 - \text{PMD})$, where the maximum allowed probability of missed detection PMD is a design parameter. The horizontal alert limit (HAL) is the maximum allowed

HPL and depends on the road network topography and can be set as half the distance between roads [14].

3. WLSR RAIM for Civil Aviation

A. Introduction

The LSR RAIM [15], together with the solution separation method [16], is one of the RAIM algorithms most frequently used in civil aviation. Moreover, the parity matrix RAIM [17] and the range comparison technique [18] are equivalent to the LSR RAIM [19]. The design of the LSR RAIM assumes that pseudorange nominal errors are modeled as independent zero-mean Gaussian distributions with the same variance. This was an acceptable condition when pseudorange errors were dominated by selective availability; however, at present, pseudorange errors are better described as independent zero-mean Gaussian distributions with variance dependent upon several factors such as signal modulation or the satellite elevation angle. In this case, the WLSR RAIM is used [20].

B. Algorithm Design the WLSR RAIM considers the following linear pseudorange measurement model

$$\Delta Y = H \cdot \Delta X + E \quad (2)$$

Where ΔY [$N_s \times 1$] is the linearized measured pseudorange vector, H [$N_s \times N_u$] is the observation matrix, ΔX [$N_u \times 1$] is the linearized navigation state vector, and E [$N_s \times 1$] is the pseudorange error vector. N_s is the number of pseudoranges, and N_u is the number of unknowns in ΔX . Two possible pseudorange error scenarios are assumed, namely, fault-free and faulty. In the fault-free case, pseudorange measurements are disturbed only by nominal errors, modeled as zero-mean independent Gaussian distributions with covariance matrix Σ . In the faulty case, apart from nominal errors, there is one biased pseudorange measurement, i.e., $E = \epsilon + B$ (3)

Where ϵ [$N_s \times 1$] is the nominal error vector, and B [$N_s \times 1$] is the bias vector. Thus

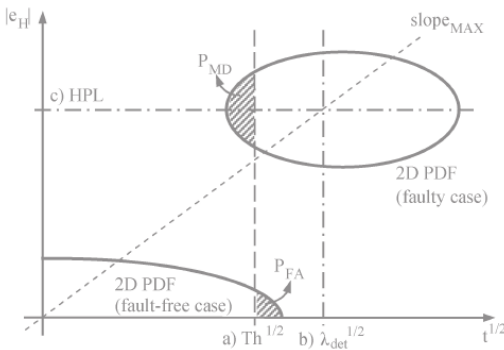
$$B = [0, \dots, b_i, 0, \dots, 0]^T \quad (4)$$

with $b_i = 0$ in the fault-free case. The probability of simultaneous faulty pseudoranges is assumed to be negligible.

The WLSR RAIM monitors the integrity of the navigation state vector calculated with the weighted least squares estimator (WLSE), i.e.,

$$\Delta \hat{X} = A \cdot \Delta Y \quad (5)$$

$$\begin{aligned} A &= (HT\Sigma \\ &-1H) \\ &-1HT\Sigma \\ &-1. \quad (6) \end{aligned}$$



The aim of RAIM algorithms is to detect positioning errors exceeding the alert limit within the required probabilities of missed and false alarm. Since positioning errors are not directly measurable, the WLSR RAIM calculates, due to the residual vector (R), a measurable scalar test statistic (t) that provides information about pseudorange measurement errors. The test statistic is computed as the weighted sum of squared errors

$$(WSSE), \text{ i.e., } t = WSSE = RT\Sigma$$

$$-1R = \Delta Y T\Sigma$$

$$-1(I - B)\Delta Y \quad (7)$$

$$R = \Delta Y - H\Delta$$

$$\bar{X} = (I - B)\Delta Y = (I - B)E \quad (8)$$

$$B = H(HT\Sigma$$

$$-1H)$$

$$-1HT\Sigma$$

$$-1. \quad (9)$$

The test statistic calculated in (7) follows a chi-squared distribution in the fault-free case and a noncentral chi-squared one in the faulty case, i.e.,

$$t \sim$$

$$\chi^2$$

$$k \text{ if } E \sim N(0, \Sigma)$$

$$\chi^2$$

$$k, \lambda \text{ if } E \sim N(B, \Sigma). \quad (10)$$

In both fault-free and faulty scenarios, the test statistic's number of degrees of freedom (k) is the number of edundant pseudo range measurements, i.e.,

$$k = N_s - N_u. \quad (11)$$

The chi-squared noncentrality parameter (λ) introduced by a faulty measurement, which depends on the bias magnitude and on the nominal errors, is

$$\lambda = (I - B)ii \cdot b^2i$$

$$/\sigma^2$$

$$i \quad (12)$$

$$\text{where } \sigma^2$$

i is the nominal error variance of the biased pseudorange, and (•)ii is the ith element of the ith row. Because we are interested in the protection against positioning failures, but the WLSR RAIM detects faults via the test statistic, the relationship between the horizontal positioning error |eH| and t needs to be investigated. In the faulty case, there is a linear relationship between the pseudorange bias projection in the horizontal error domain

(|bH|) and the square root of the test statistic λ , characterized by the slope parameter, i.e.,

$$|bH| = \text{slope}_i$$

$$\cdot$$

$$\sqrt$$

$$\lambda \quad (13)$$

$$\text{slope}_i = \sigma_i \cdot$$

$$\bar{A}2$$

$$N_i + A2$$

$$E_i$$

$$\bar{(I - B)ii} \quad (14)$$

$$\bar{(I - B)ii} \quad (14)$$

where $A2$

N_i and $A2$

E_i are the ith element of the rows of matrix in (6) corresponding to the state vector horizontal position components. The slope, which varies from one satellite to another, is an indicator of the relationship between the effect of a pseudorange bias in the test statistic and in the positioning error. A pseudorange bias leading to a given noncentrality parameter λ will have the highest impact on the positioning error when it appears in the satellite with the highest slope. The statistic components of the test statistic and the navigation state estimation errors, caused by nominal errors, are uncorrelated [21], i.e., $\text{cov}(t, e) = 0$. Therefore, the relationship between t and |eH| at a given epoch can be described as a 2-D random variable with the following probability density function (pdf):

pdf

\sqrt

t, |eH|

$\bar{=}$ pdf(

\sqrt

t) • pdf(|eH|). (15)

Once the test statistic and its relationship with the position error have been defined, the remaining RAIM parameters can be derived. These are the fault detection threshold (Th), the minimum detectable noncentrality parameter (λ_{det}), and the HPL. Fig. 1 depicts the different RAIM design process steps. In the $t^{1/2}$ against |eH| plane, in a similar way as in [22]. The bidimensional pdf has been represented by an equiprobable line for clarity reasons. Design Parameters (PMD, PFA): The WLSR RAIM is designed to meet a maximum allowed probability of missed detection (PMD) and of false detection (PFD). If the RAIM only has fault detection and not exclusion functions, any missed or false detection results in a missed or false alarm, and the maximum allowed probability of missed alarm (PMA) and false alarm (PFA) are equal to PMD and PFD, respectively. A RAIM algorithm with only a fault detection function is considered; hence, the design parameters used throughout this work are PMD and PFA. Failure Detection Threshold (Th): The WLSR RAIM detects a failure whenever the test statistic exceeds a threshold (Th). The threshold is chosen in order to assure the fault detection probability in fault-free conditions, i.e., one minus the cumulative density function (cdf) of a chi-squared function evaluated at the threshold value, i.e.,

$$PFA = p$$

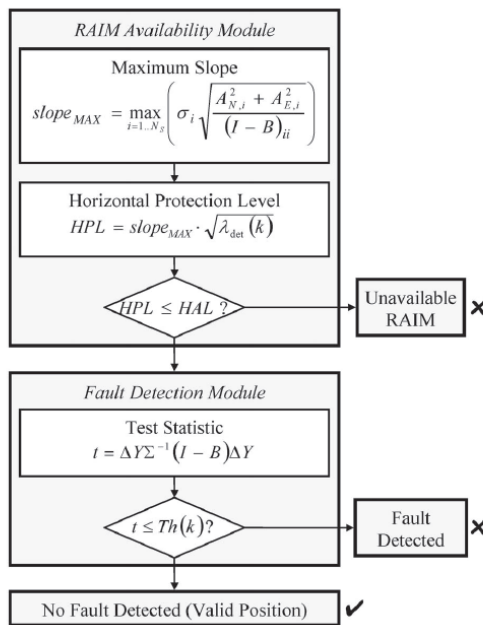
$$\begin{aligned}
 & t > Th \\
 & t \sim \chi^2_k \\
 & k = 1 - \text{cdf}\chi^2_k \\
 & \{Th\}. (16)
 \end{aligned}$$

Therefore, Th is a function of PFA and k , which, in turn, depends on the number of pseudoranges N_s .

Minimum Detectable Noncentrality Parameter (λ_{det}):

In the faulty case, the test statistic λ increases with the bias size as in (12). The minimum detectable noncentrality parameter (λ_{det}) is the λ that results in a missed detection rate equal to PMD for the threshold calculated in (16), i.e.,

$$\begin{aligned}
 & \text{PMD} = p \\
 & t \leq Th \\
 & t \sim \chi^2_k \\
 & k, \lambda_{det} \\
 & = \text{cdf}\chi^2_k \\
 & k, \lambda_{det} \\
 & \{Th\}. (17)
 \end{aligned}$$



Therefore, λ_{det} is a function of PMD, k (which depends on N_s) and Th (which also depends on PFA). HPL: The HPL is calculated as the projection in the position domain of the pseudorange bias that would generate a noncentrality parameter equal to λ_{det} in the satellite with the maximum slope ($slope_{MAX}$), i.e., $HPL = slope_{MAX} \lambda_{det}$.

$$\lambda_{det}. (18)$$

The rationale of the HPL calculation of (18) is the following. Positioning error $|e_H|$ is approximately distributed centered around $|b_H|$, if the bias is sufficiently large. Let us consider a pseudorange bias in the maximum-slope satellite with a magnitude such that the test statistic's noncentrality is equal to λ_{det} . The probability that the RAIM algorithm does not detect this pseudorange bias and that the positioning error is larger than the HPL is

approximately $PMD/2$. The probability of missed detection decreases if the biased pseudorange is in the other satellite with a lower slope. Larger biases lead to higher λ_{det} ; hence, they are always detected with a probability below PMD. Smaller bias magnitudes have smaller λ_{det} , which sets the probability nondetection over PMD. Fortunately, they also lead to lower positioning errors that offset the higher nondetection probability, resulting in a probability of missed detection of errors exceeding the HPL of less than PMD. Nevertheless, in some cases, particularly with low slopes, this may not hold [22]. C. Algorithm Implementation at the GNSS Receiver

The algorithm run within the receiver consists of two modules, i.e., the RAIM availability check and the Fault Detection (FD; see Fig. 2). The FD could be replaced by a Fault Detection and Exclusion (FDE) module.

First, at each epoch, the slope of each pseudorange measurement is calculated due to the observation matrix and the nominal error covariance matrix. The HPL is computed afterward with the maximum slope and the corresponding chi-squared noncentrality parameter. If the HPL exceeds the HAL, RAIM is not available because it cannot monitor integrity with the required HAL, i.e., PMD and PFA. In this case, the integrity cannot be monitored; hence, the estimated position is not valid for its use in ETC. If the HPL is equal to or lower than the HAL, the RAIM is available and proceeds to check whether the estimated position is faulty or not. The test statistic is computed with the linearized pseudorange measurements, the observation matrix, and the nominal error covariance matrix. If the test is higher than the corresponding detection threshold, a fault is detected, and the position cannot be used in ETC. When the test is lower than the threshold, the position is valid for ETC. The values of λ_{det} and Th depend on PMD, PFA, and the number of redundant range measurements k . They do not depend on current measurements; hence, they can be computed offline and stored in the receiver as lookup tables. The WLSR RAIM can optionally perform FDE in order to reduce service interruptions. This module tries to eliminate the biased pseudorange measurement whenever a fault is detected. If after the fault exclusion $HPL \leq HAL$ and $t \leq Th$, the position estimated without the biased pseudorange is valid for ETC. A possible fault exclusion technique creates N subgroups of $N - 1$ range measurements each; assuming that there is only one faulty pseudorange, the FD module will detect a fault in each subgroup except in the one excluding the faulty measurement. The FDE module needs at least two redundant range measurements.

4. Modified WLSR RAIM for ETC

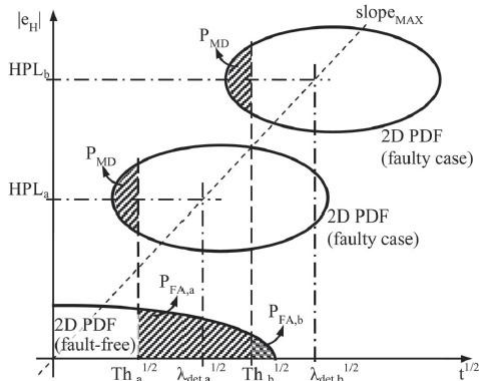
A. Motivation and Rationale of the Modified WLSR RAIM

User/satellite geometry in reduced satellite visibility scenarios such as urban environments is likely to be much worse than in the open-air scenarios commonly found in civil aviation. This fact generally increases the dilution of precision, which degrades the positioning accuracy. Another consequence of bad user/satellite geometries is the augmentation of the maximum slope, which, in turn, increases the HPL calculated as in (18), and consequently degrades the WLSR RAIM availability (which also depends on the HAL). Therefore, a GNSS-based ETC system that

monitors integrity with the WLSR RAIM in challenging environments with reduced visibility is likely to have a low number of valid positions per road segment and, consequently, a high missed geo-object recognition rate. The aim of this section is to present a modified WLSR RAIM suitable for ETC applications that improves the availability rate in environments with reduced satellite visibility without increasing the effective missed detection rate and, therefore, the toll liability risk.

According to (1), a road segment is charged to the user when the number of independent positions declared valid by the RAIM inside the geo-object is at least equal to the recognition threshold. The WLSR RAIM may not declare valid a position because it is not available or because it has detected a failure, regardless of whether it is a correct or a false detection. The aim of the modified WLSR RAIM described in this section is to maximize the number of valid positions in the fault-free scenario. The modified RAIM is designed to assure a constant PMD in order to set a known maximum probability that a faulty position inside the geo-object is declared valid when the user is actually outside it. As opposed to civil aviation, ETC systems do not require continuity; hence, their RAIM algorithms do not necessarily need to assure a maximum allowed PFA. Given constant values of PMD, slope MAX, and k, the HPL can be decreased by increasing PFA (see Fig. 3), i.e., $PFA_b < PFA_a \Rightarrow HPL_b > HPL_a$. (19)

The main idea behind the modified WLSR RAIM algorithm is to adapt PFA to the maximum slope variations to provide a tradeoff between RAIM availability and false alarms, without any restriction on the maximum allowed PFA.

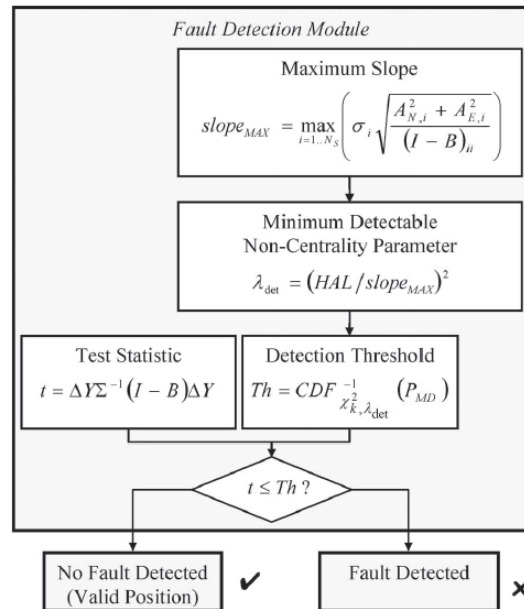


B. Algorithm Design

The objective is to design a RAIM algorithm with the WLSR test statistic described in (7) that maximizes the probability that a fault-free position (affected only by nominal errors) is declared valid, i.e., the RAIM is available and does not detect a fault. Since the WLSR test statistic is used, formulas (2)–(18) also apply to the modified WLSR RAIM. Moreover, the algorithm must assure that the probability of not detecting, in the faulty scenario, a positioning error larger than the HAL is always equal to or lower than a fixed value PMD. The first design objective is equivalent to finding the detection threshold (Th) that maximizes the probability of not detecting a failure in the

fault-free scenario, subject to the condition that the RAIM is available.

$$\begin{aligned} & \text{Thus} \\ & Th = \operatorname{argmax} \\ & Th \\ & p \\ & - \\ & t < Th \\ & - \\ & - \\ & t \sim \chi^2 \\ & k \\ & - \\ & \& (HPL \leq HAL) \end{aligned}$$



(20)
Given fixed values of PMD and k, the HPL expression of (17) is a monotonically increasing function of Th . Hence, the detection threshold that maximizes (20) is the one that results in an HPL equal to the HAL.

Therefore, the proposed RAIM procedure is designed to provide a constant HPL equal to the HAL. The minimum detectable chi-squared noncentrality parameter that corresponds to an HPL equal to HAL is derived from (18), i.e.,

$$\lambda_{det} = (HAL / slope_{MAX})^2. \quad (21)$$

The detection threshold that maximizes (20) is derived from (17) with λ_{det} calculated in (21), i.e.,

$$\begin{aligned} & Th = \operatorname{cdf}^{-1} \\ & \chi^2 \\ & k, \lambda_{det} \\ & \{PMD\}. \quad (22) \end{aligned}$$

The fault detection algorithm can already be run once the detection threshold has been calculated. For performance analysis purposes, the PFA provided at each instant can be derived from (16) with the Th calculated in (22), i.e.,

$$\begin{aligned} & PFA = 1 - \operatorname{cdf} \\ & k \end{aligned}$$

{Th}. (23)

The resulting algorithm is a constant-probability of detection RAIM [23] with the particularity of not having a maximum allowed PFA. This modified WLSR RAIM is always available (HPL = HAL); however, very high slopes lead to high false alarm probabilities. A fault-free estimated position is declared valid by the RAIM with a probability of

$$P_{\text{valid}} = 1 - \text{PFA} = \text{cdf}_{\chi^2}$$

k

(Th). (24)

C. Algorithm Implementation at the GNSS Receiver

The algorithm run at the receiver can be either the FD module (see Fig. 4) or the FDE module. There is no RAIM availability check module because the HPL is set to be always equal to the HAL.

First, at each epoch, the slope of each pseudorange measurement is computed as in the standard WLSR RAIM. Afterward, SALÓS et al.:

Since Th depends on current measurements, its exact value cannot be computed offline and stored like in the WLSR RAIM used in civil aviation. Nevertheless, it is possible to create a lookup table of Th as a function of k and discrete values of λ_{det} (for a given PMD).

Finally, the test statistic is computed as in (7) with the linearized pseudorange measurements, the observation

References

- [1] International Civil Aviation Organization (ICAO), Montreal, QC, Canada, International Standards and Recommended Practices, Annex 10 to the Convention on International Civil Aviation, Aeronautical Telecommunications, 1, Radio Navigation Aids, 2006
- [2] RTCA, Inc., Washington, DC, USA, DO-229 Minimum Operational Performance Standards for Global Positioning System/Wide Area Augmentation System Airborne Equipment, 2006, 229
- [3] Department of Defense, Arlington, VA, USA, Global Positioning Service Standard Positioning Service Performance Standard, 2008
- [4] J. Cosmen-Schortmann, M. Azaola-Saenz, M. A. Martinez-Olague, M. Toledo-Lopez, Integrity in urban and road environments and its use in liability critical applications, IEEE/ION PLANS, Monterey, CA, USA, 2008, 972–983
- [5] Racal Tracs Ltd., Chessington, U. K., Galileo Overall Architecture Definition (GALA). Definition and Sizing for The Safety of Life Market, 2000
- [6] Directive 2004/52/EC of the European Parliament and the Council on the Interoperability of Electronic Road Toll Systems in the Community, 2004
- [7] B. Pfitzinger, T. Baumann, T. Jestädt, Analysis and evaluation of the German toll system using a holistic executable specification, 45th HICSS, 2012, 5632–5638

matrix, and the nominal error covariance matrix. The estimated position is declared valid for its use in ETC if the test statistic does not exceed the threshold, and it is rejected if a fault is detected.

5. Conclusion

GNSS-based ETC systems need to monitor the positioning integrity in order to control the effects of undercharging and overcharging due to positioning failures. With this purpose, two RAIM algorithms have been studied, i.e., the WLSR RAIM used in civil aviation and a modified algorithm that, maintaining PMD, maximizes the number of valid positions (that is, available RAIM and no fault detected). The aim of the proposed algorithm is to decrease the rate of undercharging in reduced-visibility scenarios such as urban environments, assuring the same maximum allowed overcharging risk as the civil aviation RAIM procedure. This objective has been demonstrated by simulations. The improvement of dual constellation receivers in urban environments, which provide undercharging rates several orders of magnitude lower than GPS-only ones, has been also shown. The proposed design with variable PFA and a fixed HPL can be extended to other existing RAIM algorithms

- [8] R. Vargic, M. Buncak, J. Kacur, On self-similarity in service triggering in NGN networks using satellite based tolling systems, ELMAR, 2011, 183–186
- [9] N. R. Velaga, M. A. Quddus, A. L. Bristow, Y. Zheng, Map-aided integrity monitoring of a land vehicle navigation system, IEEE Trans. Intell. Transp. Syst., 13(2), 2012, 848–858
- [10] R. Toledo-Moreo, D. Betaille, F. Peyret, Lane-level integrity provision for navigation and map matching with GNSS, dead reckoning, and enhanced maps, IEEE Trans. Intell. Transp. Syst., 11(1), 2010, 100–112
- [11] R. Toledo-Moreo, M. A. Zamora-Izquierdo, B. Ubeda-Miarro, A. F. Gomez-Skarmeta, High-integrity IMM-EKF-based road vehicle navigation with low-cost GPS/SBAS/INS, IEEE Trans. Intell. Transp. Syst., 8(3), 2007, 491–511
- [12] F. van Graas, J. L. Farrell, Baseline fault detection and exclusion algorithm, 49th Annu. Meet. Inst. Navig., Cambridge, MA, USA, 1993, 413–420
- [13] International Organization for Standardization (ISO), Geneva, Switzerland, Electronic Fee Collection—Charging Performance—Part 1: Metrics, ISO/TS 17444-1, First Edition, 2012